

## Supporting Information

# Colloidal Synthesis and Optical Properties of Perovskite-Inspired Cesium Zirconium Halide Nanocrystals

Anna Abfalterer,<sup>1</sup> Javad Shamsi,<sup>1</sup> Dominik J. Kubicki,<sup>1,2</sup> Christopher N. Savory,<sup>3</sup> James Xiao,<sup>1</sup> Giorgio Divitini,<sup>4</sup> Weiwei Li,<sup>4</sup> Stuart Macpherson,<sup>1</sup> Krzysztof Gałkowski,<sup>1,5</sup> Judith L. MacManus-Driscoll,<sup>4</sup> David O. Scanlon<sup>3,6</sup> and Samuel D. Stranks<sup>1,7\*</sup>

<sup>1</sup>*Cavendish Laboratory, Department of Physics, University of Cambridge, JJ Thomson Avenue, Cambridge CB3 0HE, United Kingdom*

<sup>2</sup>*Department of Chemistry, University of Cambridge, Lensfield Road, Cambridge CB2 1EW, United Kingdom*

<sup>3</sup>*Department of Chemistry and Thomas Young Centre, University College London, 20 Gordon Street, London WC1H 0AJ, United Kingdom*

<sup>4</sup>*Department of Materials Science and Metallurgy, University of Cambridge, 27 Charles Babbage Road, Cambridge CB3 0FS, United Kingdom*

<sup>5</sup>*Institute of Physics, Faculty of Physics, Astronomy and Informatics, Nicolaus Copernicus University, 5th Grudziądzka St., 87-100 Toruń, Poland*

<sup>6</sup>*Diamond Light Source Ltd., Diamond House, Harwell Science and Innovation Campus, Didcot, Oxfordshire OX11 0DE, United Kingdom*

<sup>7</sup>*Department of Chemical Engineering and Biotechnology, University of Cambridge, Philippa Fawcett Drive, Cambridge CB3 0AS, United Kingdom*

## Corresponding Author

\*E-mail: sds65@cam.ac.uk

## Contents

1) Materials .....	3
Chemicals.....	3
2) Methods .....	4
General advice on the synthesis and handling of Cs <sub>2</sub> ZrX <sub>6</sub> (X = Cl, Br) nanocrystals (NCs).....	4
Preparation of dried ODE .....	4
Colloidal synthesis of Cs <sub>2</sub> ZrCl <sub>6</sub> NCs .....	4
Colloidal synthesis of Cs <sub>2</sub> ZrBr <sub>6</sub> NCs.....	5
Synthesis of Cs <sub>2</sub> ZrCl <sub>6</sub> bulk powder .....	5
Synthesis of Cs <sub>2</sub> ZrBr <sub>6</sub> bulk powder (with CsBr impurities).....	6
3) Characterization.....	7
Powder X-ray diffraction (XRD).....	7
Transmission electron microscopy (TEM) .....	7
Solid-state nuclear magnetic resonance (NMR) spectroscopy .....	7
Ultraviolet-visible (UV-Vis) absorption spectroscopy .....	8
Photoluminescence (PL) spectroscopy .....	9
PL quantum yield (PLQY) measurements.....	9
Time-resolved PL spectroscopy.....	10
Density functional theory (DFT) calculations .....	11
X-ray photoelectron spectroscopy (XPS) .....	11
4) Figures .....	12
Figure S1 .....	12
Figure S2.....	13
Figure S3.....	14
Figure S4.....	15
Figure S5.....	16
Figure S6.....	17
Figure S7.....	18
Figure S8.....	19
Figure S9.....	20
Figure S10.....	21
5) References .....	22

## 1) Materials

All chemical reagents were purchased from Sigma-Aldrich, stored and handled in air, and used as received unless otherwise noted. The glovebox used to store and handle chemical reagents and synthesis products in inert atmosphere was filled with argon.

### Chemicals

1-octadecene (ODE, technical grade, 90 %), zirconium(IV) acetylacetonate ( $\text{Zr}(\text{acac})_4$ , 97 %, stored in glovebox, handled in air), cesium carbonate ( $\text{Cs}_2\text{CO}_3$ , ReagentPlus®, 99 %), oleylamine (OLA, technical grade, 70 %), oleic acid (OA, technical grade, 90 %), benzoyl chloride (BzCl, ACS Reagent, 99 %, stored and handled in glovebox), toluene (anhydrous, 99.8 %, stored and handled in glovebox), benzoyl bromide (BzBr, 97 %, stored and handled in glovebox), hydrochloric acid (HCl, Honeywell Fluka, ACS reagent, 36.5-38.0 %), water ( $\text{H}_2\text{O}$ , Fisher Chemical, analytical reagent grade), hydrobromic acid (HBr, Emplura, Merck KGaA, 47 %), hexagonal boron nitride (h-BN, 99.5 %, Alfa Aesar), TEKPol (Cortecnet), 1,1,2,2-tetrachloroethane (TCE, > 98.0 %).

## 2) Methods

### General advice on the synthesis and handling of $\text{Cs}_2\text{ZrX}_6$ ( $X = \text{Cl}, \text{Br}$ ) nanocrystals (NCs)

Bulk  $\text{Cs}_2\text{ZrCl}_6$  and  $\text{Cs}_2\text{ZrBr}_6$  are hygroscopic.<sup>1-3</sup> Similarly, we also find  $\text{Cs}_2\text{ZrCl}_6$  and  $\text{Cs}_2\text{ZrBr}_6$  NCs to be very sensitive to exposure to ambient conditions. We therefore synthesize and characterize the  $\text{Cs}_2\text{ZrCl}_6$  and  $\text{Cs}_2\text{ZrBr}_6$  NCs by excluding the presence of moisture as much as possible. For example, we perform the synthesis of  $\text{Cs}_2\text{ZrX}_6$  NCs using strict air-free Schlenk line techniques. This requires quick set-up of the apparatus with hot glassware taken directly from a drying oven for both the preparation of dried ODE required for the nanocrystal (NC) synthesis as well as the  $\text{Cs}_2\text{ZrX}_6$  NC synthesis itself. Also, we transfer any liquids/suspensions between glovebox and Schlenk line set-up and vice versa by filling the liquids/suspensions into a syringe and capping the needle with an Argon-filled glass vial with septum cap to minimize air ingress.

### Preparation of dried ODE

Using Schlenk line techniques, ODE (10 mL) was dried by refluxing under vacuum for 60 minutes or 75 minutes (75 minutes for dried ODE used for the synthesis of  $\text{Cs}_2\text{ZrCl}_6$  NCs prepared with both OLA and OA ligands, 60 minutes for dried ODE used for all other NC syntheses) while magnetically stirring. Then, the system was switched to  $\text{N}_2$  atmosphere, the heating mantle removed and the dried ODE allowed to cool to room temperature. The dried ODE was transferred into the glovebox for storage until further use.

### Colloidal synthesis of $\text{Cs}_2\text{ZrCl}_6$ NCs

For the colloidal synthesis of  $\text{Cs}_2\text{ZrCl}_6$  NCs,  $\text{Zr}(\text{acac})_4$  (0.049 g, 0.10 mmol),  $\text{Cs}_2\text{CO}_3$  (0.033 g, 0.10 mmol), ODE (8.0 mL), OLA (0.60 mL), and OA (1.0 mL) were loaded into a 50 mL 3-neck round bottom flask and dried by refluxing under vacuum for 90 minutes while magnetically stirring at setting 4 on an IKA<sup>®</sup> C-MAG HS 4 S000 magnetic stirrer. The precursor salts fully dissolved. Then, a dilution of  $\text{BzCl}$  (0.20 mL) in dried ODE (1.3 mL) was swiftly injected at 185 °C into the stirred solution under  $\text{N}_2$ . 30 seconds after injection, the heating mantle was exchanged for a cold water bath and the reaction mixture allowed cooling to 30 °C. Subsequently, the cold water bath was removed, the stirring discontinued, and the colloidal suspension transferred into the glovebox. Inside the glovebox, the suspension was placed into a centrifuge tube, the tube tightly closed, taken out of the glovebox, and centrifuged at 9000 rpm (rotor radius 10.4 cm) for 15 minutes. Then, the tube was taken back into the glovebox and the supernatant discarded. The precipitate was gently rinsed with 1 mL of toluene, the supernatant discarded, and the  $\text{Cs}_2\text{ZrCl}_6$  NCs redispersed in 1 mL of fresh toluene. The colloidal suspension of  $\text{Cs}_2\text{ZrCl}_6$  NCs in toluene was stored inside the glovebox until further use.

Note, that we have had reproducibility issues with the synthesis of the  $\text{Cs}_2\text{ZrCl}_6$  NCs using the above mentioned reaction conditions. We found the synthesis of  $\text{Cs}_2\text{ZrCl}_6$  NCs to be very sensitive to solution temperatures at injection of the chloride precursor. In many cases, we did not observe NC formation by eye after injecting the mixture of  $\text{BzCl}$  in dried ODE at 185 °C. We

assume that this might have been due to a strong complex formed between OLA and  $Zr^{4+}$  ions. At 185 °C, this complex might have just been stable enough to sufficiently make  $Zr^{4+}$  unavailable for reaction with  $Cs^+$  and  $Cl^-$  ions. But upon injecting BzCl diluted in dried ODE at slightly higher temperatures (190 °C; precursor solution temperature equilibrated to 190 °C for 1 hour prior to injection), the obtained crystals were polydisperse and in parts significantly larger than 100 nm. In order to corroborate our assumption of the presence of a strong  $Zr^{4+}$ -OLA complex, we then synthesized  $Cs_2ZrCl_6$  NCs without using OLA but leaving the rest of the reaction conditions constant apart from the reaction temperature, which we changed to 190 °C (instead of 185 °C), and the time of centrifugation, which was changed to 20 minutes (instead of 15 minutes). And indeed,  $Cs_2ZrCl_6$  NCs formed with high reproducibility in all cases. Therefore, for future works, we suggest to synthesize  $Cs_2ZrCl_6$  NCs without the use of OLA.

#### Colloidal synthesis of $Cs_2ZrBr_6$ NCs

The synthesis of  $Cs_2ZrBr_6$  NCs largely followed the one of  $Cs_2ZrCl_6$  NCs except for the following differences. For the colloidal synthesis of  $Cs_2ZrBr_6$  NCs, no OLA was used, BzBr (0.60 mL) diluted in dried ODE (0.90 mL) was injected into the solution stirred at setting 6 (increased from setting 4 shortly before injection), and the  $Cs_2ZrBr_6$  NCs were redispersed in 2 mL of fresh toluene instead of 1 mL. The synthesis of  $Cs_2ZrBr_6$  NCs with two additional washing steps adds the following procedure to the original synthesis recipe of  $Cs_2ZrBr_6$  NCs: centrifuging the NC suspension at 9000 rpm for 15 minutes (rotor radius 10.4 cm), discarding the supernatant, rinsing the precipitate with 1 mL toluene, discarding the supernatant, redispersing the NCs in 2 mL toluene (2x). All these additional steps were performed under exclusion of air and moisture.

#### Synthesis of $Cs_2ZrCl_6$ bulk powder

For the synthesis of  $Cs_2ZrCl_6$  bulk powder, we followed a published method with slight modifications to the Zr and Cs precursors, reactant concentrations, and drying temperature and duration.<sup>4</sup> Specifically,  $Zr(acac)_4$  (0.294 g, 0.603 mmol) was dissolved in 5.0 mL HCl under stirring.  $Cs_2CO_3$  (0.195 g, 0.598 mmol) was dissolved in 0.40 mL  $H_2O$  under stirring. Then, the solution of  $Zr(acac)_4$  in HCl was pipetted into the solution of  $Cs_2CO_3$  in  $H_2O$  while stirring. A suspension formed immediately. The stirring was continued for 10 minutes, then the suspension centrifuged at 3000 rpm (rotor radius 10.4 cm) for 3 minutes, and the supernatant discarded. The following washing steps were repeated twice. HCl (2.0 mL) was added to the precipitate, the precipitate resuspended, the suspension centrifuged at 3000 rpm (rotor radius 10.4 cm) for 3 minutes, and the supernatant discarded. Then, the precipitate was placed in a glass vial, the vial heated to 150 °C on a hot plate and kept at that temperature for 90 minutes. Subsequently, the hot vial with the dried  $Cs_2ZrCl_6$  bulk powder was quickly transferred into the glovebox for storage until further use. It is important to wear appropriate gloves to transfer the hot vial.

*Synthesis of Cs<sub>2</sub>ZrBr<sub>6</sub> bulk powder (with CsBr impurities)*

For the synthesis of Cs<sub>2</sub>ZrBr<sub>6</sub> bulk powder, Zr(acac)<sub>4</sub> (0.587 g, 1.20 mmol) was dissolved in HBr (0.60 mL) under stirring. Cs<sub>2</sub>CO<sub>3</sub> (0.195 g, 0.598 mmol) was placed in a round bottom flask and dissolved in 0.10 mL H<sub>2</sub>O under stirring. Both solutions were placed in a water-ice bath and allowed to equilibrate in temperature for 10 minutes before the Zr(acac)<sub>4</sub> in HBr solution was pipetted into the solution of Cs<sub>2</sub>CO<sub>3</sub> in H<sub>2</sub>O while stirring. After a few seconds, a suspension formed. The stirring was continued for 20 minutes at 0 °C, then the suspension centrifuged at 3000 rpm (rotor radius 10.4 cm) for 3 minutes at room temperature, and the supernatant discarded. The following washing step was performed once and only with a small amount of HBr, as addition of larger amounts of HBr dissolves the product. HBr (0.20 mL) was added to the precipitate, the precipitate resuspended, the suspension centrifuged at 3000 rpm (rotor radius 10.4 cm) for 3 minutes, and the supernatant discarded. Then, the precipitate was placed on a petri dish, the petri dish heated to 150 °C on a hot plate and kept at that temperature for 30 minutes. Subsequently, the hot petri dish with the dried product was quickly transferred into the glovebox for storage until further use. It is important to wear appropriate gloves to transfer the hot petri dish.

### 3) Characterization

#### Powder X-ray diffraction (XRD)

Powder XRD measurements were collected on a Bruker D8 Discover diffractometer in  $\theta$ - $\theta$  configuration equipped with a Cu K $_{\alpha}$  tube (40 kV, 40 mA, average wavelength = 1.5418 Å) and a Bruker LYNXEYE XE detector. Sample rotation was on during measurements. The XRD measurements were performed in air-free conditions using an air-free sample holder. Therefore, the samples were prepared inside the glovebox. Cs<sub>2</sub>ZrX<sub>6</sub> NC thin film samples were fabricated by drop-casting the colloidal suspensions of Cs<sub>2</sub>ZrCl<sub>6</sub> NCs on a Si substrate and of Cs<sub>2</sub>ZrBr<sub>6</sub> NCs on a glass substrate. Cs<sub>2</sub>ZrX<sub>6</sub> bulk powders were placed on glass substrates for the XRD measurements.

#### Transmission electron microscopy (TEM)

TEM images of Cs<sub>2</sub>ZrX<sub>6</sub> NCs were collected on a FEI Tecnai F20 field emission gun TEM. The acceleration voltage was 200 kV. The TEM samples were prepared by drop-casting dilutions of the Cs<sub>2</sub>ZrX<sub>6</sub> NC suspensions onto 300 Mesh copper TEM grids with carbon films, respectively, inside the glovebox. The TEM grids with Cs<sub>2</sub>ZrCl<sub>6</sub> NC samples were triple-bagged in plastic bags inside the glovebox for transport to the TEM instrument. The grids were exposed to the ambient for about 2 to 3 minutes before they were loaded into the vacuum system of the TEM instrument. The TEM grids with Cs<sub>2</sub>ZrBr<sub>6</sub> NC samples were loaded into the TEM without exposure to the ambient using a Gatan double tilt air-free transfer holder (Model 648).

#### Solid-state nuclear magnetic resonance (NMR) spectroscopy

Room temperature <sup>133</sup>Cs (91.8 MHz) magic angle spinning (MAS) NMR spectra were recorded on a Bruker Avance III 16.4 T spectrometer equipped with a 4.0 mm CPMAS probe. <sup>133</sup>Cs (78.7 MHz), <sup>13</sup>C (150.9 MHz) and <sup>15</sup>N (60.8 MHz) dynamic nuclear polarization (DNP)-enhanced MAS NMR spectra were recorded on a Bruker Avance III 14.1 T spectrometer equipped with a 3.2 mm LTMAS probe. <sup>13</sup>C and <sup>15</sup>N spectra were referenced based on the unified IUPAC scale for referencing, using solid adamantane as a secondary reference (<sup>13</sup>C  $\delta$ =29.456 ppm).<sup>5</sup> <sup>133</sup>Cs shifts were referenced using solid CsI as a secondary reference ( $\delta$ =271.05 ppm).<sup>6</sup>

For conventional room temperature MAS NMR experiments, the samples were packed into gas-tight zirconia rotors inside an argon glovebox. About 250 mg (full 4 mm rotor) of Cs<sub>2</sub>ZrCl<sub>6</sub> bulk powder was used. For the Cs<sub>2</sub>ZrCl<sub>6</sub> NC sample, a colloidal suspension of Cs<sub>2</sub>ZrCl<sub>6</sub> NCs was placed into a centrifuge tube inside the glovebox, the tube tightly closed, taken out of the glovebox, and centrifuged at 9000 rpm (rotor radius 10.4 cm) for 15 minutes. Then, the tube was taken back into the glovebox and the supernatant discarded. Overnight, the tube was kept inside the glovebox without lid to allow residual toluene to evaporate. This process yielded about 2 mg of dry solid NCs. Note that the Cs<sub>2</sub>ZrCl<sub>6</sub> NCs used for the conventional room temperature MAS NMR experiments were made with slight deviations from the above mentioned synthesis recipe for Cs<sub>2</sub>ZrCl<sub>6</sub> NCs (using both OLA and OA as ligands) with the changes being the use of 14 mL ODE (instead of 8 mL) and a Cs-oleate precursor (instead of Cs<sub>2</sub>CO<sub>3</sub> directly), a degassing

duration of 60 minutes (instead of 90 minutes), injection of the BzCl in ODE mixture at setting 2 (instead of 4) and centrifugation of the NCs for 25 minutes (instead of 15 minutes).

For MAS DNP experiments, the colloidal suspension of Cs<sub>2</sub>ZrCl<sub>6</sub> NCs was mixed with h-BN inside a glovebox and kept for 7 hours at 50-54 °C on a hot plate to dry the sample and then another 2 days at room temperature inside the glovebox to allow the sample to fully dry. About 50 mg of the resulting solid mixture was wetted with 12 μL of a 17 mM TEKPol solution in TCE in a fume hood. During this wetting process, the sample got exposed to ambient air conditions for about two minutes. Subsequently, it was transferred into a 3.2 mm sapphire rotor and frozen at 100 K under nitrogen inside the NMR probe.

The acquisition and processing parameters are given below:

Composition	Experiment	Recycle delay [s]	Number of scans	Acquisition time [h]	Lorentzian apodization [Hz]
Cs <sub>2</sub> ZrCl <sub>6</sub> Bulk	<sup>133</sup> Cs echo	1000	4	1.1	20
Cs <sub>2</sub> ZrCl <sub>6</sub> NCs	<sup>133</sup> Cs Bloch decay	40	1200	13.3	50 (main signal) 500 (surface sites)
Cs <sub>2</sub> ZrCl <sub>6</sub> NCs	<sup>1</sup> H- <sup>13</sup> C CP (DNP, μW off)	9	44	0.1	100
	<sup>1</sup> H- <sup>13</sup> C CP (DNP, μW on)	9	4	0.01	100
Cs <sub>2</sub> ZrCl <sub>6</sub> NCs	<sup>1</sup> H- <sup>15</sup> N CP (DNP, μW on)	5	6120	8.5	400
Cs <sub>2</sub> ZrCl <sub>6</sub> NCs	<sup>1</sup> H- <sup>133</sup> Cs CP (with DNP, μW on), 100 K	8	128	0.28	400
Cs <sub>2</sub> ZrCl <sub>6</sub> NCs	<sup>133</sup> Cs echo (without DNP, μW off), 100 K	5	4	0.006	100

#### Ultraviolet-visible (UV-Vis) absorption spectroscopy

UV-Vis absorption measurements were performed on a Shimadzu UV-3600 Plus double-beam spectrophotometer. To prepare the encapsulated Cs<sub>2</sub>ZrX<sub>6</sub> NC thin film samples, colloidal suspensions (a dilution of a colloidal suspension for measurement of Cs<sub>2</sub>ZrBr<sub>6</sub> NCs) were drop-cast onto fused silica substrates and encapsulated by a fused silica substrate and UV-curable glue inside the glovebox. The reference sample was a stack of two fused silica substrates encapsulated with UV-curable glue. For UV-Vis measurements of the Cs<sub>2</sub>ZrBr<sub>6</sub> NC suspension in toluene, the Cs<sub>2</sub>ZrBr<sub>6</sub> NC suspension was further diluted with toluene, placed in a quartz cuvette inside the glovebox and the cuvette sealed air-tight with a stopper. The reference sample was a toluene-filled quartz cuvette.

### Photoluminescence (PL) spectroscopy

PL and PL excitation (PLE) measurements were performed on an Edinburgh Instruments FLS980 PL spectrometer. To prepare the encapsulated pure  $\text{Cs}_2\text{ZrCl}_6$  and  $\text{Cs}_2\text{ZrBr}_6$  NC thin film samples, colloidal suspensions (a dilution of a colloidal suspension for measurement of  $\text{Cs}_2\text{ZrBr}_6$  NCs) were drop-cast onto fused silica substrates and encapsulated by a fused silica substrate and UV-curable glue inside the glovebox. To prepare the encapsulated mixed  $\text{Cs}_2\text{ZrCl}_6$  and  $\text{Cs}_2\text{ZrBr}_6$  NC thin film samples, parts of a colloidal suspension of OA-only  $\text{Cs}_2\text{ZrCl}_6$  NCs were added to a diluted colloidal suspension of  $\text{Cs}_2\text{ZrBr}_6$  NCs, and the resulting suspension drop-cast onto a fused silica substrate. The film was subsequently encapsulated by a second fused silica substrate and UV-curable glue inside the glovebox. Encapsulated  $\text{Cs}_2\text{ZrX}_6$  bulk powder samples were prepared by placing the powders between two fused silica substrates and encapsulating them with UV-curable glue inside the glovebox. The  $\text{Cs}_2\text{ZrBr}_6$  NC suspension in toluene sample was prepared by diluting the  $\text{Cs}_2\text{ZrBr}_6$  NC suspension in toluene in a quartz cuvette inside the glovebox and sealing the cuvette air-tight with a stopper. All PL spectra are corrected for instrument response. The PL spectra of the mixed  $\text{Cs}_2\text{ZrCl}_6$  and  $\text{Cs}_2\text{ZrBr}_6$  NC thin film sample and the  $\text{Cs}_2\text{ZrBr}_6$  NC suspension in toluene were additionally background corrected for a PL measurement of a stack of two fused silica substrates encapsulated with UV-curable glue and a PL measurement of a toluene-filled quartz cuvette, respectively. Excitation was at 250 nm and 248 nm for encapsulated  $\text{Cs}_2\text{ZrCl}_6$  NC thin film and bulk powder samples, respectively, at 300 nm and 320 nm for encapsulated  $\text{Cs}_2\text{ZrBr}_6$  NC thin film and bulk powder samples, respectively, at 250 nm for the encapsulated mixed  $\text{Cs}_2\text{ZrCl}_6$  and  $\text{Cs}_2\text{ZrBr}_6$  NC thin film samples, and at 300 nm for the  $\text{Cs}_2\text{ZrBr}_6$  NC suspension in toluene. All PLE spectra are corrected for instrument response and PLE spectra of the  $\text{Cs}_2\text{ZrBr}_6$  NC thin film sample and mixed  $\text{Cs}_2\text{ZrCl}_6$  and  $\text{Cs}_2\text{ZrBr}_6$  NC thin film samples are background corrected for a PLE measurement of a stack of two fused silica substrates encapsulated with UV-curable glue.

### PL quantum yield (PLQY) measurements

PLQY measurements on  $\text{Cs}_2\text{ZrBr}_6$  samples were performed with the integrating sphere method on an Edinburgh Instruments FLS980 fluorescence spectrometer with F-M01 integrating sphere attachment.<sup>7</sup> Excitation was provided with a 450 W CW xenon lamp monochromated at 300 nm with a 5 nm bandwidth. The detector was a R928 photomultiplier tube monochromated from 290 – 800 nm (280-820 nm) with 1 nm (0.2 nm) bandwidth and 0.5 nm (0.1 nm) step size for the champion  $\text{Cs}_2\text{ZrBr}_6$  NC thin film sample (all other samples).  $\text{Cs}_2\text{ZrBr}_6$  NC thin film samples were prepared by drop-casting a dilution of the colloidal suspension of  $\text{Cs}_2\text{ZrBr}_6$  NCs onto a fused silica substrate and encapsulating by another fused silica substrate and UV-curable glue inside the glovebox.  $\text{Cs}_2\text{ZrBr}_6$  powder samples were prepared by placing a spatula tip of powder onto a fused silica substrate, pressing it flat with another fused silica substrate and encapsulating the two substrates with UV-curable glue inside the glovebox. The  $\text{Cs}_2\text{ZrBr}_6$  NC suspension samples were prepared by diluting  $\text{Cs}_2\text{ZrBr}_6$  NC suspension in toluene in a quartz cuvette and sealing the cuvette air-tight with a stopper inside the glovebox. For PLQY measurements of

Cs<sub>2</sub>ZrBr<sub>6</sub> NC thin films and Cs<sub>2</sub>ZrBr<sub>6</sub> powders, a stack of two fused silica substrates encapsulated with UV-curable glue (for the champion Cs<sub>2</sub>ZrBr<sub>6</sub> NC thin film measurement, but two stacks for all other measurements) were used as a blank and to verify that there was no additional emission from the encapsulant. For PLQY measurements of Cs<sub>2</sub>ZrBr<sub>6</sub> NC suspensions, two quartz cuvettes filled with toluene and capped with stoppers were used as the blanks. PL spectra, including the excitation wavelength, were measured with the samples in direct, indirect and blank excitation conditions. The recorded spectra were corrected for spectral response of the integrating sphere-monochromator-detector system. Integrals of the excitation peak and emission peak in each measurement condition were taken and the PLQY values were calculated as follows:

$$\eta = \frac{E_D(PL_I) - E_I(PL_D)}{(E_D - E_I)E_B}$$

where E<sub>B</sub>, E<sub>D</sub>, E<sub>I</sub> are the integrals of the excitation peak in the blank, direct and indirect sample excitation conditions, respectively. PL<sub>D</sub> and PL<sub>I</sub> are the integrals of the photoluminescence peak in the direct and indirect sample excitation conditions, respectively.

A total of 2, 3, and 5 PLQY measurements were performed on Cs<sub>2</sub>ZrBr<sub>6</sub> powders, NC suspensions and NC thin films, respectively, on 2, 2, and 3 sample batches, respectively, to account for PLQY measurement variation due to sample preparation and variation between sample batches. The reported values of the two PLQY measurements of Cs<sub>2</sub>ZrBr<sub>6</sub> powders and the three PLQY measurements of Cs<sub>2</sub>ZrBr<sub>6</sub> NC suspensions are averages. The averages including the standard deviations  $\sigma$  ( $\sigma = \frac{\sqrt{\sum(x_i - \mu)^2}}{N}$ , x<sub>i</sub> being the PLQY value for each measurement and  $\mu$  the average PLQY) for these PLQY measurements are 44 ± 5 % (N=2) for Cs<sub>2</sub>ZrBr<sub>6</sub> powders and 40 ± 8 % (N=3) for Cs<sub>2</sub>ZrBr<sub>6</sub> NC suspensions. The reported 45 % PLQY value in the main text is the champion value for our Cs<sub>2</sub>ZrBr<sub>6</sub> NC thin film samples. Typical thin film PLQY values are 22 ± 2 % (N=4), but significant light outcoupling effects have to be considered for these measurements and will contribute to the observed differences in PLQY. We also note that our champion thin film PLQY was achieved from a film deposited from a NC suspension stored in inert conditions for 4 months.

#### Time-resolved PL spectroscopy

Time-resolved PL was collected using a gated intensified CCD camera (Andor iStar DH740 CCI-010) connected to a calibrated grating spectrometer (Andor SR303i). The 800 nm emission from a Ti:sapphire optical amplifier (1 kHz repetition rate, 90 fs pulse width) was frequency-doubled to generate narrow bandwidth excitation centred at a wavelength of 400 nm. The incident beam was focused to an effective Gaussian diameter of 200 μm and had an average power of 800 μW, yielding an energy per pulse of ~2,500 μJ/cm<sup>2</sup>, sufficient for considerable two-photon absorption within the sample. The encapsulated Cs<sub>2</sub>ZrBr<sub>6</sub> NC thin film sample was the same one as for the champion thin film PLQY measurements.

### Density functional theory (DFT) calculations

DFT calculations were performed on  $\text{Cs}_2\text{ZrCl}_6$  and  $\text{Cs}_2\text{ZrBr}_6$  within periodic boundary conditions using the Vienna Ab Initio Simulation Package (VASP).<sup>8-11</sup> The projector augmented wave method was used to describe the interaction between valence and core electrons,<sup>12</sup> with all pseudopotentials being scalar-relativistic, and both 4p and 4s electrons were included as valence in the Zr pseudopotential. As discussed in the article, the hybrid functional HSE06, incorporating 25 % Hartree-Fock exchange at short range, governed by the range separation parameter of 0.11 bohr<sup>-1</sup>,<sup>13</sup> was used to describe the exchange-correlation potential in all calculations. Hybrid DFT is an apt method to accurately describe the band gap and single-particle optical properties<sup>14</sup> of semiconductors, and HSE06 has been used to accurately describe such properties for other closed d-shell systems,<sup>15-18</sup> as well as structurally-related ‘defect perovskite’ structures that include octahedra separated by interstitial space.<sup>19</sup> For all electronic structure and optical calculations, spin-orbit coupling was also included (HSE06+SOC). Additional calculations were performed using HSE06 (omitting SOC) and the PBE functional<sup>20</sup> to quantify the relativistic renormalisation of the band gap of  $\text{Cs}_2\text{ZrCl}_6$  (0.10 eV), and to assess the necessity of using a hybrid functional, respectively. The band gap of  $\text{Cs}_2\text{ZrCl}_6$  using PBE alone was 3.76 eV, a significant underestimate of the experimental UV-Vis absorption onset, hence all calculations in the remainder of the work use the more accurate and appropriate HSE06+SOC method. A plane wave cutoff energy of 400 eV and a Gamma-centred k-point mesh of 4x4x4 were found to converge the total energy of both compounds to within 1 meV per atom, and so were used for electronic calculations; during relaxation of the structure to its equilibrium positions, the cutoff energy was increased to 560 eV to avoid Pulay stress.<sup>21</sup> The relaxation was determined to be converged once the force on all atoms was below 0.01 eV per Å, and the total energy was converged to within 10<sup>-5</sup> eV for all calculations. Convergence of the optical spectrum with respect to k-mesh was tested up to 10x10x10 with minimal change in the real or imaginary dielectric function. The plotting of density of states (DOS), band structures and optical properties was possible through the use of the sumo package,<sup>22</sup> and the Gelius weighting and broadening of the DOS for comparison with XPS used the open-source software galore,<sup>23</sup> using photoionization cross-sections from Yeh and Lindau<sup>24</sup> – this dataset does not provide cross-sections for Cs 6s orbitals, however these states are negligibly present in the valence band of  $\text{Cs}_2\text{ZrCl}_6$ .

### X-ray photoelectron spectroscopy (XPS)

XPS measurements were performed on a Thermo Scientific Escalab 250 Xi spectrometer with a monochromatic Al K<sub>α</sub> X-ray source (1486.7 eV). The  $\text{Cs}_2\text{ZrCl}_6$  NC thin film sample was prepared by drop-casting 10 μL of the colloidal suspension of  $\text{Cs}_2\text{ZrCl}_6$  NCs onto a Si substrate (~1x1 cm) inside the glovebox. Then, the substrate was attached to the XPS sample holder with Cu tape. The holder was placed into a plastic bag for transport from the glovebox to the XPS instrument and quickly transferred into the vacuum system of the XPS instrument to limit the exposure of the sample to ambient conditions to about 15 seconds.

#### 4) Figures

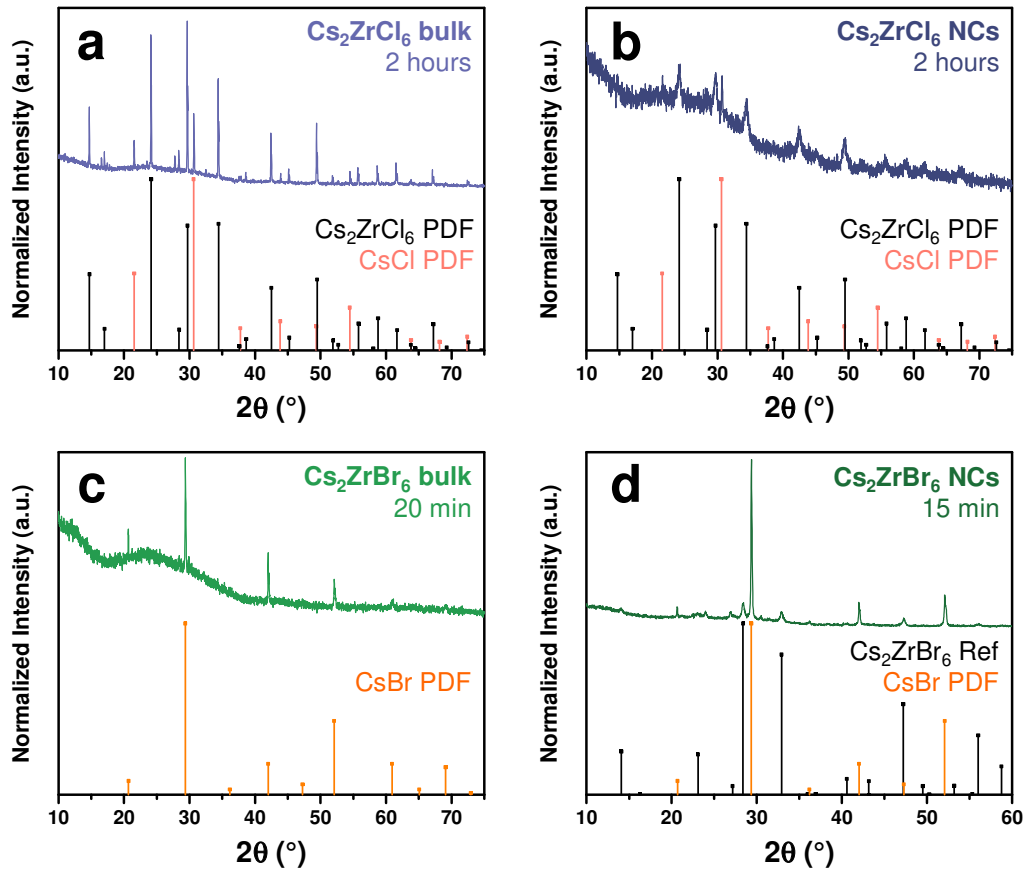


Figure S1: (a), (b) XRD patterns of  $\text{Cs}_2\text{ZrCl}_6$  (a) bulk powder (light blue) and (b) NC thin film (blue) samples that were each exposed to ambient air conditions for about 2 hours as well as reference XRD patterns of  $\text{Cs}_2\text{ZrCl}_6$  (PDF 01-074-1001; black)<sup>25</sup> and  $\text{CsCl}$  (PDF 00-005-0607; red)<sup>26</sup>. (c), (d) XRD patterns of  $\text{Cs}_2\text{ZrBr}_6$  (c) bulk powder (including  $\text{CsBr}$  phase impurity; light green) and (d) NC thin film (green) samples that were exposed to ambient air conditions for about 20 min and 15 min, respectively, as well as reference XRD patterns of  $\text{Cs}_2\text{ZrBr}_6$  (black) and  $\text{CsBr}$  (PDF 00-005-0588; orange)<sup>27</sup>. (a)-(d) The samples were prepared on glass substrates, which introduce a broad background between  $\sim 17^\circ$  and  $38^\circ$ . The diffraction patterns are normalized to their respective maximum intensity and vertically offset for clarity.

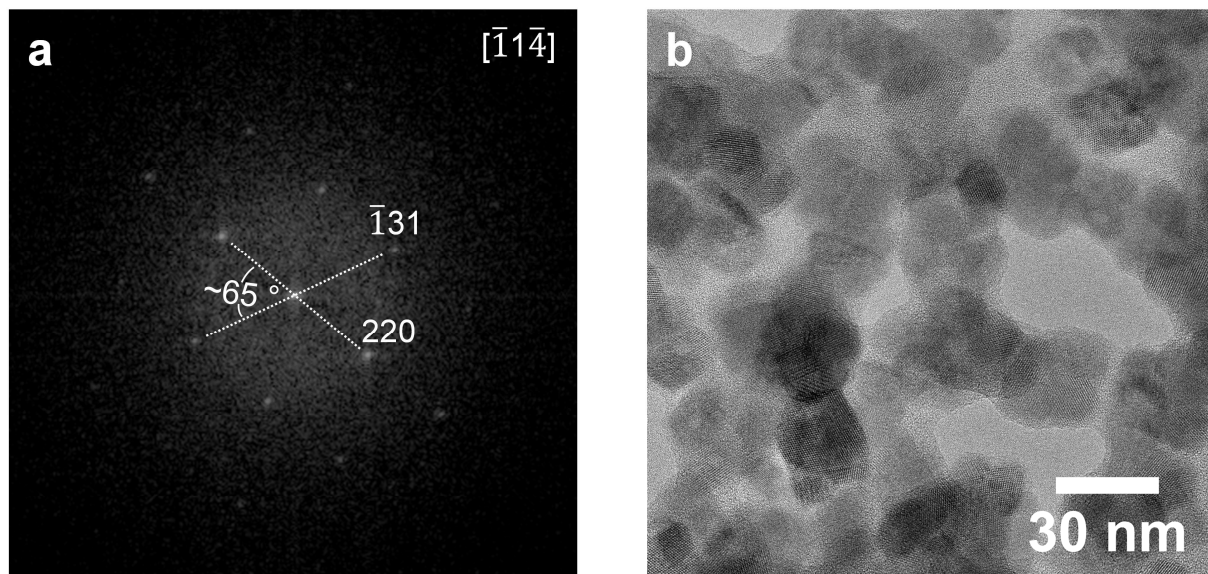


Figure S2: (a) Fast Fourier transform (FFT) of the high-resolution TEM (HR-TEM) image of the  $\text{Cs}_2\text{ZrCl}_6$  NC shown in the inset of Figure 1c. The FFT reflections match diffraction spots of the powder diffraction file of  $\text{Cs}_2\text{ZrCl}_6$  (PDF 01-074-1001)<sup>25</sup>. The  $(\bar{1}31)$  and  $(220)$  reflections are indexed. They include a  $65^\circ$  angle with the origin. The zone axis is down  $[\bar{1}1\bar{4}]$ . (b) Larger area HR-TEM image of  $\text{Cs}_2\text{ZrCl}_6$  NCs. We note that we cannot exclude the presence of other phases due to potential beam damage and exposure of the sample to ambient conditions during sample loading.

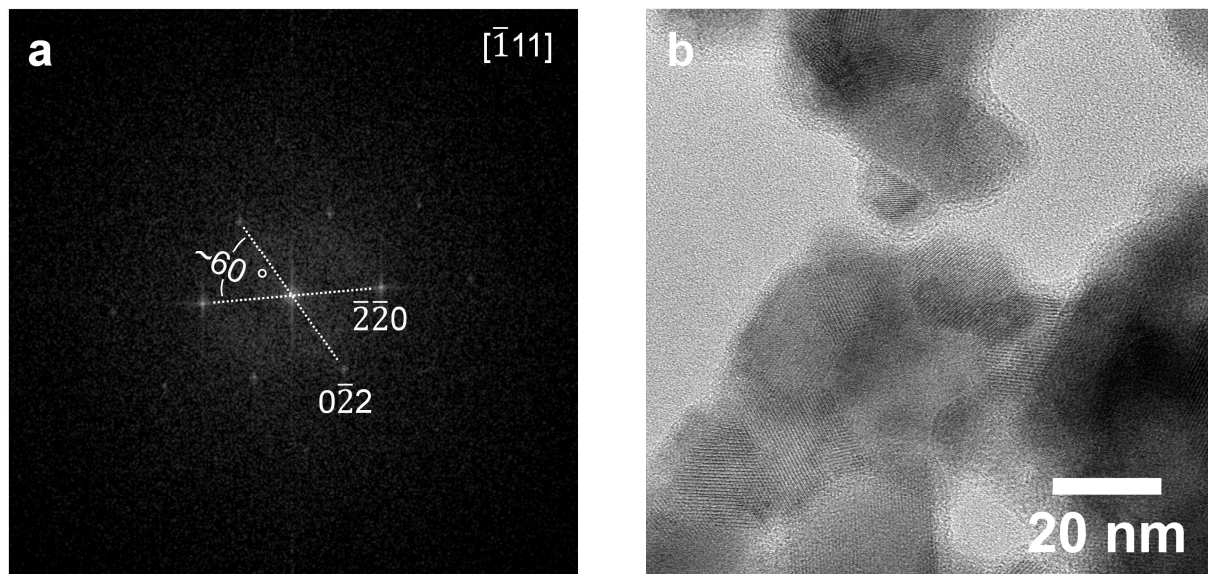


Figure S3: (a) FFT of the HR-TEM image of the  $\text{Cs}_2\text{ZrBr}_6$  NC shown in the inset of Figure 1d. The FFT reflections match diffraction spots of the simulated reference XRD pattern of  $\text{Cs}_2\text{ZrBr}_6$ . The  $(\bar{2}\bar{2}0)$  and  $(0\bar{2}2)$  reflections are indexed. They include a  $60^\circ$  angle with the origin. The zone axis is down  $[\bar{1}11]$ . (b) Larger area HR-TEM image of  $\text{Cs}_2\text{ZrBr}_6$  NCs. We note that we cannot exclude the presence of other phases due to potential beam damage.

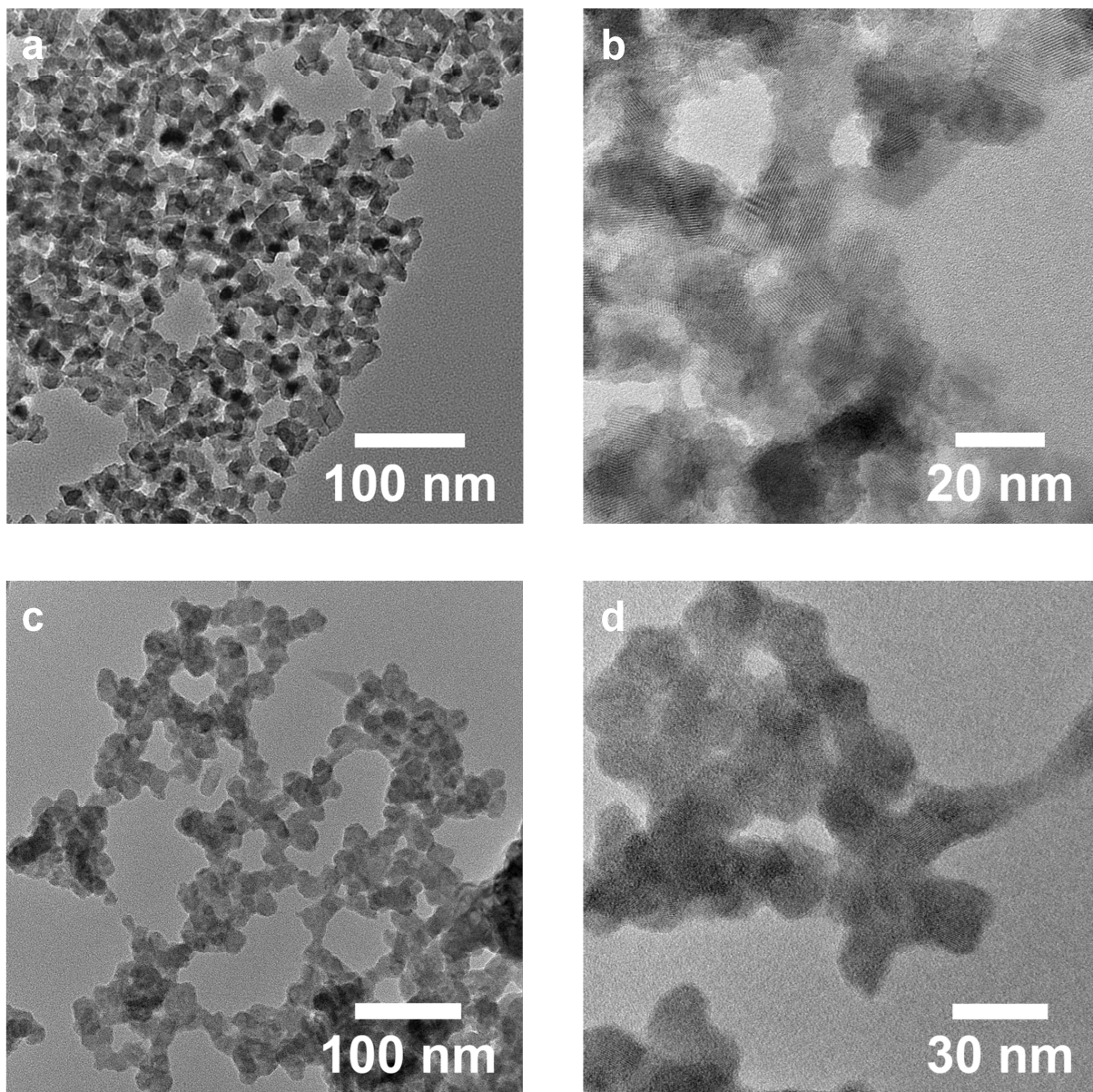


Figure S4: (a) TEM image and (b) HR-TEM image of Cs<sub>2</sub>ZrBr<sub>6</sub> NCs prepared with two additional washing steps. (c) TEM image and (d) HR-TEM image of oleate-capped Cs<sub>2</sub>ZrCl<sub>6</sub> NCs. We note that phases other than Cs<sub>2</sub>ZrX<sub>6</sub> cannot be excluded in the HR-TEM images due to potential beam damage and exposure of the Cs<sub>2</sub>ZrCl<sub>6</sub> NC sample to ambient conditions during sample loading.

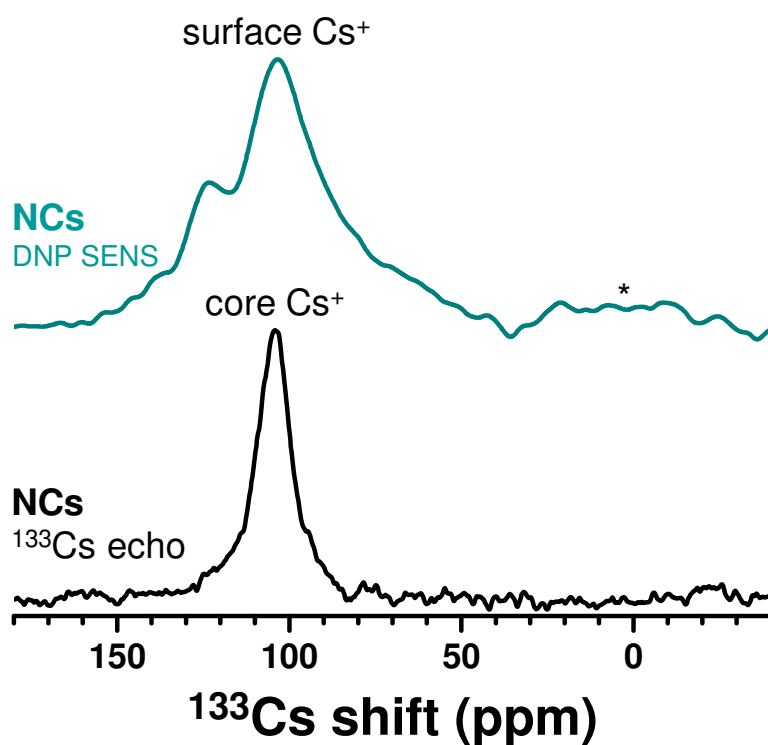


Figure S5: DNP SENS characterization of  $\text{Cs}_2\text{ZrCl}_6$  NCs. Solid-state MAS NMR spectra at 14.1 T, 100 K and 10 kHz MAS of  $\text{Cs}_2\text{ZrCl}_6$  NCs formulated with h-BN and wetted with 17 mM TEKPol in TCE. At the top is the surface-enhanced  $^1\text{H}$ - $^{133}\text{Cs}$  CP spectrum preferentially showing the surface  $\text{Cs}^+$  sites (recorded with microwave irradiation). At the bottom is the echo-detected  $^{133}\text{Cs}$  spectrum highlighting the core  $\text{Cs}^+$  sites (recorded without microwave irradiation). The asterisk indicates a spinning sideband. The spectra are vertically offset for clarity.

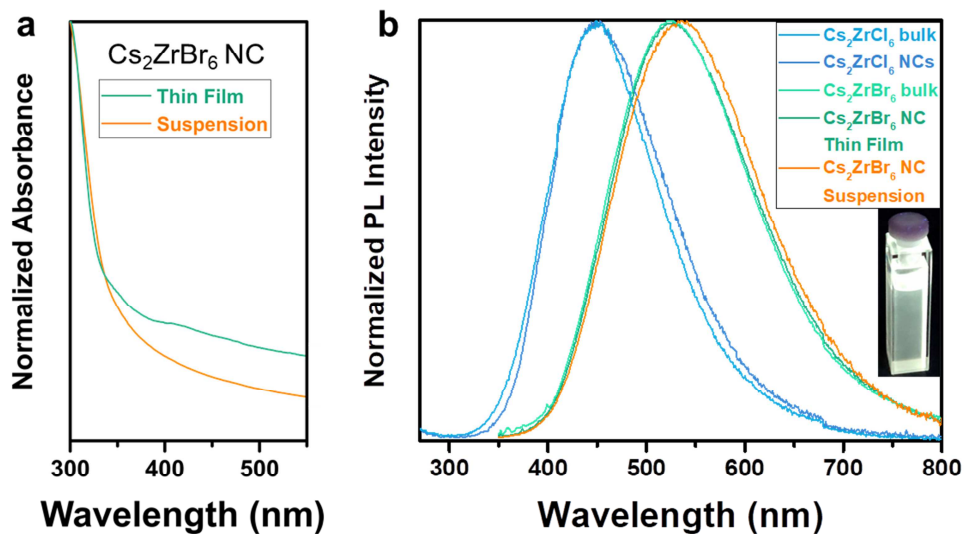


Figure S6: (a) UV-Vis absorption spectra of an encapsulated Cs<sub>2</sub>ZrBr<sub>6</sub> NC thin film sample (green) and a Cs<sub>2</sub>ZrBr<sub>6</sub> NC suspension in toluene sample (orange). (b) PL spectra of encapsulated Cs<sub>2</sub>ZrCl<sub>6</sub> (blue) and Cs<sub>2</sub>ZrBr<sub>6</sub> (green) NC thin film samples, encapsulated Cs<sub>2</sub>ZrCl<sub>6</sub> (light-blue) and Cs<sub>2</sub>ZrBr<sub>6</sub> (light-green) bulk powder samples and a Cs<sub>2</sub>ZrBr<sub>6</sub> NC suspension in toluene sample (orange). The excitation was at 250 nm and 248 nm for encapsulated Cs<sub>2</sub>ZrCl<sub>6</sub> NC thin film and powder samples, respectively, and at 300 nm, 300 nm and 320 nm for encapsulated Cs<sub>2</sub>ZrBr<sub>6</sub> NC thin film, NC suspension and powder samples, respectively. The inset shows a picture of a cuvette filled with Cs<sub>2</sub>ZrBr<sub>6</sub> NC suspension in toluene under 254 nm UV-light irradiation. All spectra shown in (a) and (b) are normalized to their respective maximum intensity.

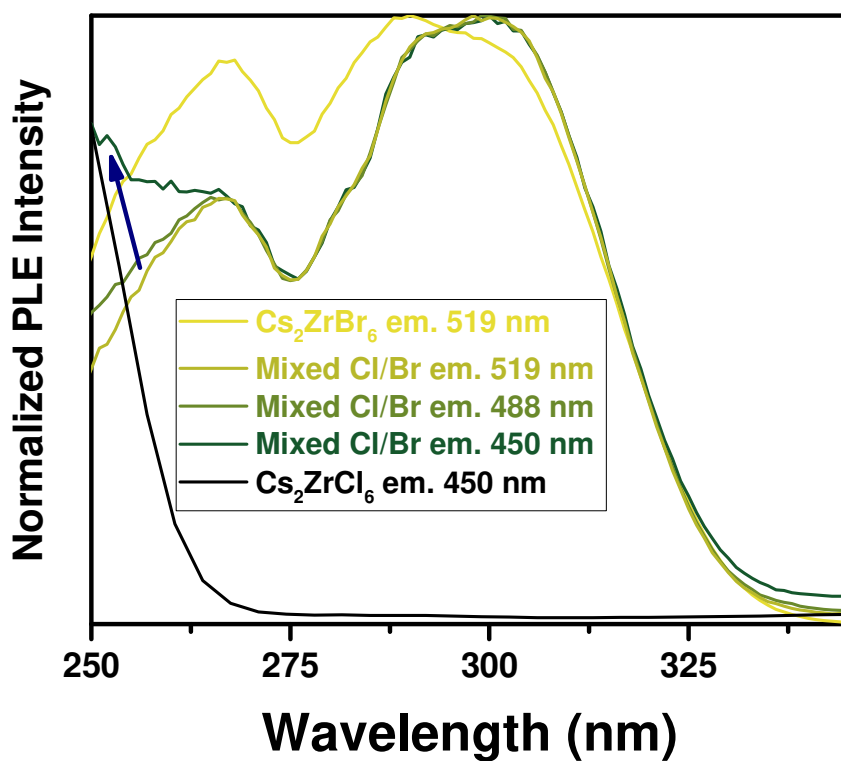


Figure S7: PLE spectra of a mixed  $\text{Cs}_2\text{ZrCl}_6$  and  $\text{Cs}_2\text{ZrBr}_6$  NC encapsulated thin film for emission wavelengths of 450, 488, and 519 nm in comparison to the PLE spectra of pure  $\text{Cs}_2\text{ZrCl}_6$  and  $\text{Cs}_2\text{ZrBr}_6$  NC thin films for emission at 450 nm and 519 nm, respectively. The spectra are normalized to their respective maximum intensity. The arrow indicates a contribution from  $\text{Cs}_2\text{ZrCl}_6$  to the PL for higher emission energies (450 nm) in mixed  $\text{Cs}_2\text{ZrCl}_6$  and  $\text{Cs}_2\text{ZrBr}_6$  NC thin films, while at lower emission energies (519 nm) the emission is due to excitation of  $\text{Cs}_2\text{ZrBr}_6$ . We note that the pure  $\text{Cs}_2\text{ZrCl}_6$  NC sample used to measure the black PLE curve was made using Cs-oleate as the Cs-source.

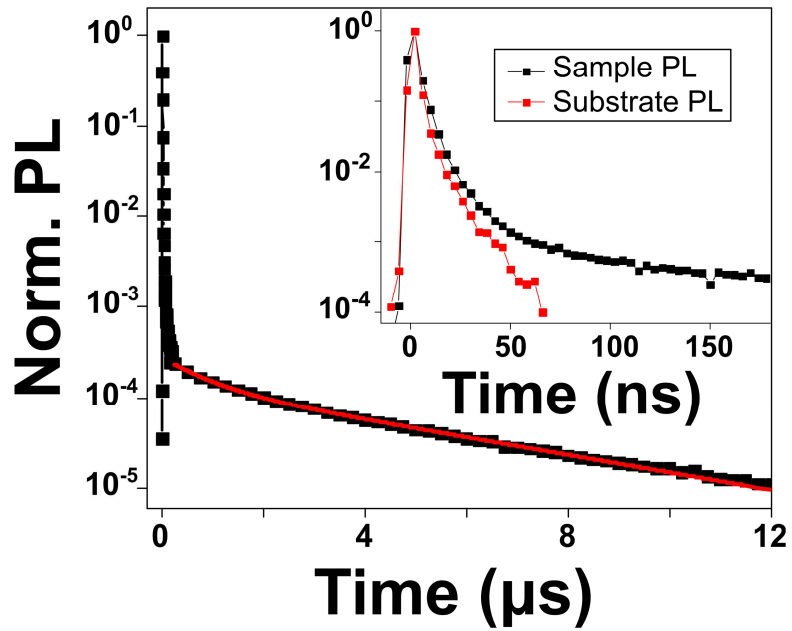


Figure S8: Spectrally integrated PL decay of an encapsulated  $\text{Cs}_2\text{ZrBr}_6$  NC thin film (black curve). The red line is a double-exponential fit of the long-lived decay components of the experimental data, with time constants of  $\tau_1 = 780 \pm 40$  ns (amplitude  $A_1 = 1.03 \times 10^{-4}$ ) and  $\tau_2 = 4500 \pm 100$  ns (amplitude  $A_2 = 1.34 \times 10^{-4}$ ). Inset: Zoom of the early time PL decay of the encapsulated sample (black curve) in comparison to the decay of the substrate only (red curve). We attribute this fast initial component to emission from the substrate, and the longer components to the sample decay.

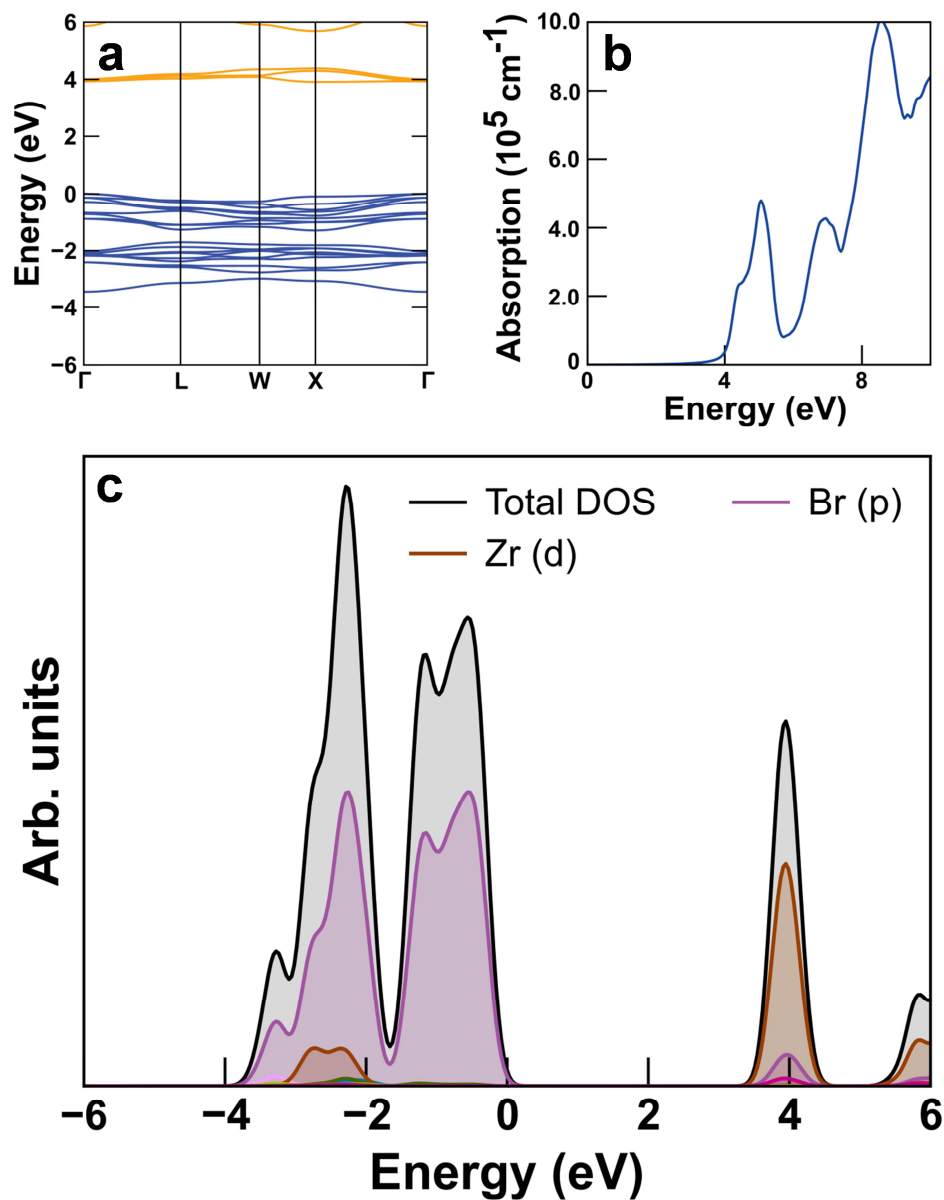


Figure S9: Electronic and optical properties calculated using HSE06+SOC on  $\text{Cs}_2\text{ZrBr}_6$ : (a) electronic band structure, with valence band in blue and conduction bands in orange, and the valence band maximum set to 0 eV; (b) optical absorption coefficient; (c) density of states, with valence band maximum set to 0 eV and orbital contributions lower than 1% omitted from legend for clarity.

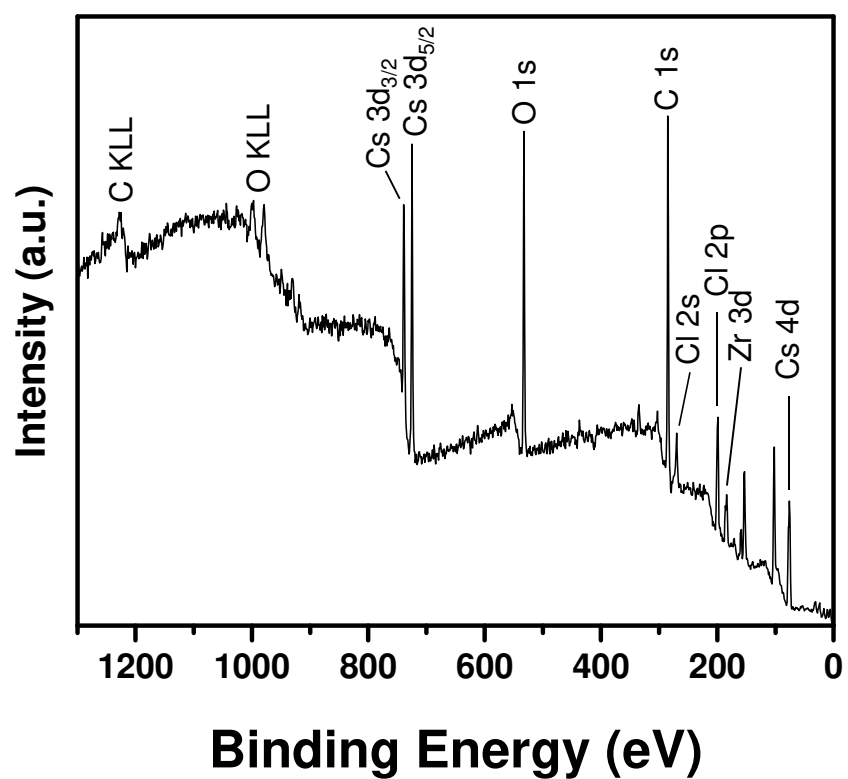


Figure S10: Survey XPS scan of a  $\text{Cs}_2\text{ZrCl}_6$  NC thin film. We attribute the peaks at 102, 153, and 159 eV to originate from surface contamination, because we are unable to assign them to Cs, Zr or Cl.

## 5) References

- (1) Metcalf, D. H.; Dai, S.; Del Cul, G. D.; Toth, L. M. Luminescence Spectra of Single Crystals of  $\text{Cs}_2\text{ZrCl}_6:\text{UO}_2\text{Cl}_4^{2-}$  at Low Temperatures. Vibronic Structure of  $\text{UO}_2^{2+}$  Doped in a Cubic Host. *Inorg. Chem.* **1995**, *34*, 5573–5577. <https://doi.org/10.1021/ic00126a030>.
- (2) Xu, W.; Dai, S.; Toth, L. M.; Peterson, J. R. Blue Up-Conversion Emission from  $\text{U}^{4+}$ -Ion Doped into  $\text{Cs}_2\text{ZrCl}_6$  Single Crystal under Green Light ( $19436\text{ cm}^{-1}$ ) Excitation. *Chem. Phys.* **1995**, *193*, 339–344. [https://doi.org/10.1016/0301-0104\(94\)00393-O](https://doi.org/10.1016/0301-0104(94)00393-O).
- (3) Aebischer, A.; Salley, G. M.; Güdel, H. U. Near Infrared to Visible Photon Upconversion in  $\text{Re}^{4+}$  Doped  $\text{Cs}_2\text{ZrBr}_6$ . *J. Chem. Phys.* **2002**, *117*, 8515–8522. <https://doi.org/10.1063/1.1513455>.
- (4) Drummen, P. J. H.; Donker, H.; Smit, W. M. A.; Blasse, G. Jahn-Teller Distortion in the Excited State of Tellurium(IV) in  $\text{Cs}_2\text{MCl}_6$  (M=Zr, Sn). *Chem. Phys. Lett.* **1988**, *144*, 460–462. [https://doi.org/10.1016/0009-2614\(88\)87296-8](https://doi.org/10.1016/0009-2614(88)87296-8).
- (5) Morcombe, C. R.; Zilm, K. W. Chemical Shift Referencing in MAS Solid State NMR. *J. Magn. Reson.* **2003**, *162*, 479–486. [https://doi.org/10.1016/S1090-7807\(03\)00082-X](https://doi.org/10.1016/S1090-7807(03)00082-X).
- (6) Hayashi, S.; Hayamizu, K. Accurate Determination of NMR Chemical Shifts in Alkali Halides and Their Correlation with Structural Factors. *Bull. Chem. Soc. Jpn* **1990**, *63*, 913–919. <https://doi.org/10.1246/bcsj.63.913>.
- (7) deMello, J. C.; Wittmann, H. F.; Friend, R. H. An Improved Experimental Determination of External Photoluminescence Quantum Efficiency. *Adv. Mater.* **1997**, *9*, 230–232. <https://doi.org/10.1002/adma.19970090308>.
- (8) Kresse, G.; Hafner, J. Ab Initio Molecular Dynamics for Liquid Metals. *Phys. Rev. B* **1993**, *47*, 558–561. <https://doi.org/10.1103/PhysRevB.47.558>.
- (9) Kresse, G.; Hafner, J. Ab Initio Molecular-Dynamics Simulation of the Liquid-Metal--Amorphous-Semiconductor Transition in Germanium. *Phys. Rev. B* **1994**, *49*, 14251–14269. <https://doi.org/10.1103/PhysRevB.49.14251>.
- (10) Kresse, G.; Furthmüller, J. Efficiency of Ab-Initio Total Energy Calculations for Metals and Semiconductors Using a Plane-Wave Basis Set. *Comput. Mater. Sci.* **1996**, *6*, 15–50. [https://doi.org/10.1016/0927-0256\(96\)00008-0](https://doi.org/10.1016/0927-0256(96)00008-0).
- (11) Kresse, G.; Furthmüller, J. Efficient Iterative Schemes for Ab Initio Total-Energy Calculations Using a Plane-Wave Basis Set. *Phys. Rev. B* **1996**, *54*, 11169–11186. <https://doi.org/10.1103/PhysRevB.54.11169>.
- (12) Blöchl, P. E. Projector Augmented-Wave Method. *Phys. Rev. B* **1994**, *50*, 17953–17979. <https://doi.org/10.1103/PhysRevB.50.17953>.
- (13) Krukau, A. V.; Vydrov, O. A.; Izmaylov, A. F.; Scuseria, G. E. Influence of the Exchange Screening Parameter on the Performance of Screened Hybrid Functionals. *J. Chem. Phys.* **2006**, *125*, 224106. <https://doi.org/10.1063/1.2404663>.
- (14) Gajdoš, M.; Hummer, K.; Kresse, G.; Furthmüller, J.; Bechstedt, F. Linear Optical Properties in the Projector-Augmented Wave Methodology. *Phys. Rev. B* **2006**, *73*, 045112. <https://doi.org/10.1103/PhysRevB.73.045112>.
- (15) Deák, P.; Aradi, B.; Frauenheim, T. Polaronic Effects in  $\text{TiO}_2$  Calculated by the HSE06 Hybrid Functional: Dopant Passivation by Carrier Self-Trapping. *Phys. Rev. B* **2011**, *83*, 155207. <https://doi.org/10.1103/PhysRevB.83.155207>.
- (16) Sathasivam, S.; Williamson, B. A. D.; Kafizas, A.; Althabaiti, S. A.; Obaid, A. Y.; Basahel, S. N.; Scanlon, D. O.; Carmalt, C. J.; Parkin, I. P. Computational and Experimental Study

- of Ta<sub>2</sub>O<sub>5</sub> Thin Films. *J. Phys. Chem. C* **2017**, *121*, 202–210.  
<https://doi.org/10.1021/acs.jpcc.6b11073>.
- (17) Birkett, M.; Savory, C. N.; Fioretti, A. N.; Thompson, P.; Muryn, C. A.; Weerakkody, A. D.; Mitrovic, I. Z.; Hall, S.; Treharne, R.; Dhanak, V. R.; Scanlon, D. O.; Zakutayev, A.; Veal, T. D. Atypically Small Temperature-Dependence of the Direct Band Gap in the Metastable Semiconductor Copper Nitride Cu<sub>3</sub>N. *Phys. Rev. B* **2017**, *95*, 115201.  
<https://doi.org/10.1103/PhysRevB.95.115201>.
- (18) Padilha, A. C. M.; McKenna, K. P. Structure and Properties of a Model Conductive Filament/Host Oxide Interface in HfO<sub>2</sub>-Based ReRAM. *Phys. Rev. Mater.* **2018**, *2*, 045001.  
<https://doi.org/10.1103/PhysRevMaterials.2.045001>.
- (19) Maughan, A. E.; Ganose, A. M.; Bordelon, M. M.; Miller, E. M.; Scanlon, D. O.; Neilson, J. R. Defect Tolerance to Intolerance in the Vacancy-Ordered Double Perovskite Semiconductors Cs<sub>2</sub>SnI<sub>6</sub> and Cs<sub>2</sub>TeI<sub>6</sub>. *J. Am. Chem. Soc.* **2016**, *138*, 8453–8464.  
<https://doi.org/10.1021/jacs.6b03207>.
- (20) Perdew, J. P.; Burke, K.; Ernzerhof, M. Generalized Gradient Approximation Made Simple. *Phys. Rev. Lett.* **1996**, *77*, 3865–3868. <https://doi.org/10.1103/PhysRevLett.77.3865>.
- (21) Pulay, P. Ab Initio Calculation of Force Constants and Equilibrium Geometries in Polyatomic Molecules. *Mol. Phys.* **1969**, *17*, 197–204.  
<https://doi.org/10.1080/00268976900100941>.
- (22) Ganose, A. M.; Jackson, A. J.; Scanlon, D. O. Sumo: Command-Line Tools for Plotting and Analysis of Periodic Ab Initio Calculations. *J. Open Source Softw.* **2018**, *3*, 717.  
<https://doi.org/10.21105/joss.00717>.
- (23) Jackson, A. J.; Ganose, A. M.; Regoutz, A.; Egdell, R. G.; Scanlon, D. O. Galore: Broadening and Weighting for Simulation of Photoelectron Spectroscopy. *J. Open Source Softw.* **2018**, *3*, 773. <https://doi.org/10.21105/joss.00773>.
- (24) Yeh, J. J.; Lindau, I. Atomic Subshell Photoionization Cross Sections and Asymmetry Parameters:  $1 \leq Z \leq 103$ . *At. Data Nucl. Data Tables* **1985**, *32*, 1–155.  
[https://doi.org/10.1016/0092-640X\(85\)90016-6](https://doi.org/10.1016/0092-640X(85)90016-6).
- (25) Engel, G. Die Kristallstrukturen Einiger Hexachlorokomplexsalze. *Z. Kristallogr. Cryst. Mater.* **1935**, *90*, 341–373. <https://doi.org/10.1524/zkri.1935.90.1.341>.
- (26) Swanson, H. E.; Fuyat, R. K. Standard X-Ray Diffraction Powder Patterns. *Natl. Bur. Stand. (U.S.)* **1953**, *Circular 539*, 2, 44.
- (27) Swanson, H. E.; Fuyat, R. K.; Ugrinic, G. M. Standard X-Ray Diffraction Powder Patterns. *Natl. Bur. Stand. (U.S.)* **1954**, *Circular 539*, 3, 49.